5th Australasian Congress on Applied Mechanics, ACAM 2007

10-12 December 2007, Brisbane, Australia

Wear Transitions in a Wear Coefficient Model

T.T. Vuong and P.A. Meehan

Department of Mechanical Engineering, The University of Queensland

Abstract: The frictional-work wear model has been used popularly for the prediction of wear phenomena such as rail corrugation. The accuracy of such models depends on the value chosen for the empirical wear coefficient in this wear model. Experimental results have widely shown that this wear coefficient is strongly dependent upon the type of wear process involved.

The wear coefficient in the frictional-work wear model under two-disc contact and dry friction conditions proposed is a multi-step function of the friction power density corresponding to three types of wear. However, at present there is no clear means of predicting the transitions between wear types.

This paper investigates wear transitions between the wear types are predicted using analytical models based on the wear mechanics involved.

Keywords: Load factor, Shakedown limit, Asperity, Bulk temperature, Flash temperature

1. Introduction

In twin-disc test of rail materials, three wear types have been defined well in terms of wear rate, disc contact surface appearance, metallographic features of disc sections and wear debris: type I (mild wear), type II (severe wear) and type III wear (catastrophic wear), shown in [1], [4] [19] and [22]. The results from [1] and [19] showed that at the transition between each wear type a distinct change in wear rate occurs. Two wear transition areas between type I and II and between type II and III have been confirmed in [17-19], [5], [4], [1] and [7].

The wear rate -a wear quantity- can be represented by a wear coefficient (k_0) in the frictional-work wear model ($\Delta m = k_0.\Delta W$, here Δm and ΔW are the mass loss and friction work respectively). The wear coefficient can be a piece-wise constant character function of energy flow density, with an emphasised jump at a certain value of energy flow density, where the transition occurs [23].

Several experimental investigations have been carried out to determine the wear coefficient and wear transition. The value of wear coefficients depends on the contact surface material and wear types, for a certain material pair the value of wear coefficient for wear type I and II is approximately constant and linear for wear type III (see [2] and [22]). The wear rate and the wear transition area between wear type II and type III for some wheel/rail steels also has been illuminated by experiment results in [17], [19], [1], [4] and [7].

By combining the recent experimental results in literature, ref. [22] has suggested a general model for the wear coefficient. The general model is a multi-step function of the friction power density corresponding to three types of wear. This paper investigates the wear transition by suggesting the analytical models for the friction power density (E_{I-II} and E_{II-III}), where the wear transition occurs.

2. Determination of the first wear transition area from type I to type II (E_{I-II})

The experiment results show that the wear transition between type I and type II occurs when the partial slip reaches full slip [18], [17] and the load reaches the shakedown limit [1]. Based on these two conditions, this section will suggest an equation for determining the wear transition area from type I to type II wear.

2.1. Influence of the slip state on wear transition

In twin-disc contact, the contact area is assumed to be elliptical. The contact area includes an area of slip and an area of adhesion (or stick). If the traction force is less than the limiting friction force, the contact is in a state of partial slip. When the traction force is equal to the limiting friction force, the stick area disappears and the contact is in a state of full slip [13]. On the other hand, the states of slip can be shown by the creep curve as Figure 1.

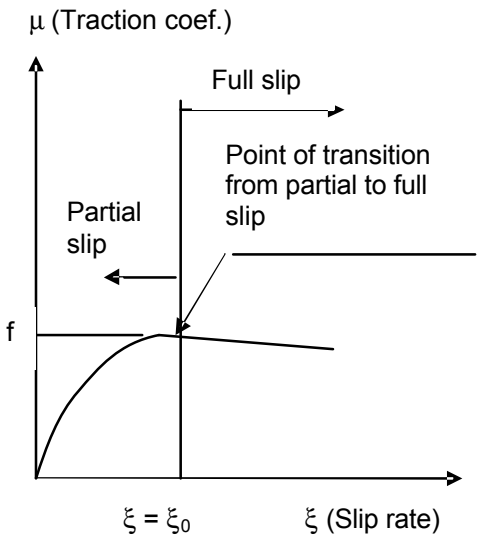

Figure 1: The Creep Curve

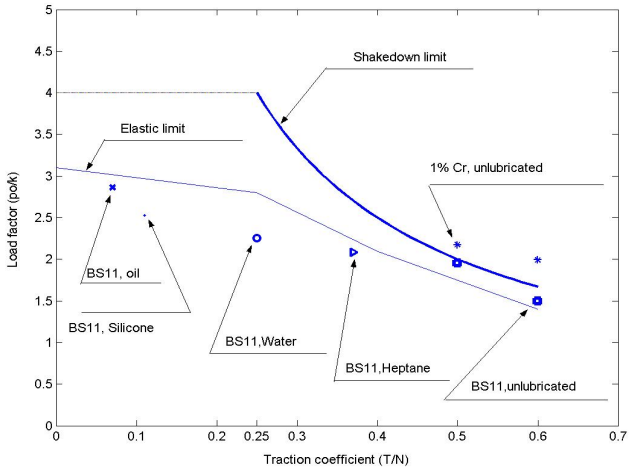

Figure 2: Wear transition points on the shakedown diagram

In the creep curve, at the point of transition from partial slip to full slip, the traction coefficient is equal to the limiting friction coefficient (f) and the slip rate is equal to the limiting slip rate (ξ_0).

Investigating the influence of slip on the wear transition for twin-disc contact, Lewis [18], [17] has confirmed that wear transition from type I to type II is associated with the onset of fully sliding contact condition. This condition can be shown by the following equation: $\xi = \xi_0$ (1)

2.2. Influence of load on wear transition

The influence of load on the wear behaviour and wear transition can be shown by the 'shakedown diagram' (see [11], [1] and [8]).

The shakedown diagram represents the coordinates of traction coefficient (μ) and the load factor (p_0/k), in which p_0 is the maximum Hertz contact pressure and k is the yield stress in simple shear. The 'shakedown limit' (p^s_0) in the diagram is a criterion of material that has often been used when studying rolling contact stresses. Below the shakedown limit, two behaviours observed are perfectly elastic and 'elastic shakedown'. Above the shakedown limit, two behaviours observed are 'plastic shakedown' and 'ratchetting' [13],[14], [10].

Figure 2, derived from the data in [1], describe the relationship between load factor and traction coefficient when wear transitions occurring, in which ' ', '>', 'o', '.', 'x' corresponds to the wear transition points for BS11 rail steel under the conditions unlubricated, lubricated by water, lubricated by oil ('lardedge'), lubricated by Heptane and lubricated by silicone fluid respectively; and '*' corresponds to the wear transition points for 1% Chrome steel under unlubricated conditions.

Figure 2 showed that under dry friction (unlubricated) conditions, the wear transition occurs when the load factor (p_0/k) approached the limit load factor (p^s_0/k). Approximately, it can be assumed that the wear transition between type I and type II occurs when the maximum Hertz contact pressure (p_0) reaches to the shakedown limit (p^s_0).

Based on the characteristic of the shakedown diagram in the rolling/sliding contact [13] and [14], the contact pressure (p_0), corresponding to the wear transition is determined by the following equations.

$p_0/k \approx 4$, if $\mu < 0.25$ and $p_0/k = 1/\mu$, if $\mu \geq 0.25$

For twin-disc contact, the range of limited friction coefficients is often between 0.4 and 0.5 for dry friction condition [8]. When full slip occurs, the traction coefficient is often more than 0.25. Therefore the relationship between the load and the traction coefficient can be selected as, $p_0/k = 1/\mu$ (2)

2.3. An equation to determine the transition area I-II

The friction power density (P_r / A_n) can be determined by the following equation,

$P_r / A_n = T V_s / A_n = \mu (N/A_n)\xi V = \mu.(p_m)\xi V = \mu (\pi p_0/4)\xi V$ (3)

Where T is the traction force, V is the nominal rolling velocity, V_s is the relative slip velocity, N is the normal force, A_n is the nominal contact area, ξ is the creepage rate and p_m is the average contact pressure ($=\pi\ p_0/4$ for line contact [13]).

If the $E_{I\text{-}II}$ is the value of the P_r / A_n when the wear transition between type I and type II occurs, based on equations (1), (2) and (3),

$$E_{I\text{-}II} = k\ (\pi/4)\ \xi_0\ V \tag{4}$$

Here, k is the yield stress in simple shear of disc surface material and the ξ_0 is the limiting creep rate determined from the creep curve of contact material pair. In general, the $E_{I\text{-}II}$ depends on the property of contact surface material, the relative slip speed and the limiting creep rate between two surfaces.

3. Determination of the second wear transition area from type II to type III ($E_{II\text{-}III}$)

The presence of a wear transition between type II and type III has been confirmed from the experiment results in [4], [7], [17] and [19].

What wear mechanism dominates for type III wear has not been determined clearly yet. However, for the transition area II-III, the main cause leading to the wear transition may be the high surface temperature [4], and [18]. These temperatures (from 200 to 300°C) may cause a drop in the yield strength of carbon manganese steels, such as those found in wheel and rail steels [6], [18] and [21].

An equation describing the relationship between the friction power density and contact surface temperature is a necessary tool to investigate this wear transition area.

3.1. Disc surface temperature

The disc surface temperature, T_{tot}, is considered to be made up of three components, the bulk, flash and initial temperature [18].The bulk temperature, T_b, of material under the contacting surfaces of the discs, is the average temperature of the outer surface of the discs. The instantaneous temperature rise above the bulk temperature at the asperities of contact is called the flash temperature, T_f, [3], [20]. The initial temperature of the contact surface, T_0, selected conveniently as the ambient temperature.

The following sections will suggest the equations that determine the bulk temperature, flash temperature and the disc surface temperature in the cases where a significant oxide layer is present and where an oxide layer is not present on the contact surface.

3.1.1. The bulk temperature

In the literature there have been some surface temperature models suggested for real wheel-rail contact [9], pin-on-disc contact [20] and twin-disc contact [17]. To facilitate a comparison with available experimental data, the temperature model for twin-disc contact has been selected to investigate this wear transition area.

In general, in order to calculate the bulk temperature, T_b, of the twin-disc contact, heat generated due to sliding friction in the contact is assumed to be equal to heat loss due to convection, conduction and radiation. The results of temperature calculation for the twin-disc wear test in [17] show that the proportion of radiation and convection heat dissipated is very low compared to conduction heat generated (see Table 3 in [17]). Therefore the radiation and convection heat loss can be neglected.

The heat dissipated due to conduction can be determined from Equation (4) in [17] for twin-disc contact, however, this equation includes the T_i (temperature at a r_i radius) that depends on the size of the test discs. Therefore it would not be generally applicable to different experimental cases. A general approach used in [16] and [9] for determining real wheel/rail contact bulk temperature would be more appropriate for applying here.

When the surface temperature of wheel and rail disc are equal everywhere in the contact area, the risen bulk temperature (ΔT_b) due to the heat supply within the contact patch can be determined by the thermal equations in [9].

$$\Delta T_b = 0.836\ \frac{\varepsilon\mu V_s p_0}{\beta_w}\left(\frac{a}{V_w}\right)^{0.5} = 0.836\ \frac{(1-\varepsilon)\mu V_s p_0}{\beta_r}\left(\frac{a}{V_r}\right)^{0.5} \tag{5}$$

Where, ε is the heat partitioning factor, μ is the traction coefficient, $\beta_{w,r}$ is the thermal penetration coefficient of wheel and rail steel respectively, the a is the semi-contact-width of contact area, $V_{w,r}$ is

the rolling velocity of the wheel and rail disc respectively, V_s is the relative slip speed between two contact surfaces and p_0 is the maximum Hertz contact pressure.

As $V_s = V_w - V_r = \xi . V_w$; $\beta_w = \beta_r = \beta_{steel} = 13290$ ($W.s^{0.5}/K.m^2$) and ε is determined as the part of frictional heating that flows into the wheel disc, in similar way as in [9] and [3],

$e = \left(b_w \sqrt{V_w} \right) / \left(b_w \sqrt{V_w} + b_r \sqrt{V_r} \right)$. Based on equations (3) and (5),

$$\Delta T_b = 8 \times 10^{-5} \left(\frac{1}{1 + \sqrt{1 - x}} \right) \left(\frac{a}{V_w} \right)^{0.5} \frac{P_r}{A_n} \tag{6}$$

For the line contact [13], $a/R = 2.p_0/E^*$ (7)

Where, R is the equivalent radius of contact surface pair, a is semi-contact-width of contact area and E^* is the equivalent Young's modulus. For the steel, Young's modulus, $E=2.1.10^{11}$ (Pa) and the Poison coefficient $\nu=0.3$, E^* equals to $1.17.10^{11}$ (Pa). Inserting (7) into (6) with $E^*_{steel} = 1.17 \times 10^{11}$(Pa),

$$\Delta T_b = 1.65 \times 10^{-10} \left(\frac{\sqrt{p_0}}{1 + \sqrt{1 - x}} \right) \left(\sqrt{\frac{R}{V_w}} \right) \left(\frac{P_r}{A_n} \right) \tag{8}$$

Equation (8) shows that the rise in bulk surface temperature is not only proportional to the frictional power density but also on the contact pressure and creepage rate. The bulk temperature T_b is,

$T_b = \Delta T_b + T_0$ (9)

T_0 is the initial temperature of the contact surface, selected conveniently as the ambient temperature.

3.1.2. The flash temperature

The flash temperature (T_f) is the instantaneous temperature rise above the bulk temperature at the "asperities" in contact, defined in [3] and [20].

Ref. [20] suggested that the frictional heat is really generated at the tiny contact areas ("asperities") which make up the true area of contact at the sliding interface. The rise in instantaneous temperature of these contact points can be higher than the rise in bulk temperature (ΔT_b).

When a non-dimensional parameter (L), similar to the Peclet number, that may be interpreted as the ratio of the surface speed to the rate of diffusion of heat into the solid [13], is enough high (L > 5), based on the thermal equations in [17], the flash temperature for line contact can be deduced by,

$$T_f = \frac{(P_r / A_n)}{\lambda} \left(\frac{2 c a}{\pi V} \right)^{0.5} \tag{10}$$

Where V is the velocity of either contact solid, which can be selected as a nominal rolling speed ($V=V_w$). The λ is the thermal conductivity coefficient, which for steel is approximately calculated by $\lambda = \lambda_s = 50$ (W/m.K) and χ (m^2/s) is the thermal diffusivity coefficient, defined as $\chi = \lambda/(\rho C_p)$. In which C_p is the specific heat capacity, which for steel is calculated by $C_p = C_{ps} = 450$ (J/kg.K) and $\rho = 7850$ (kg/m^3) is the density for steel.

When the influence of the oxide layer on the contact surface can be neglected, selecting $\lambda = \lambda_s$, equation (10) becomes,

$$T_f = 5.1 \times 10^{-5} \left(\frac{a}{V_w} \right)^{0.5} \frac{P_r}{A_n} \quad \text{, Or, } T_f = 2.1 \times 10^{-10} \left(\sqrt{p_0} \right) \left(\sqrt{\frac{R}{V_w}} \right) \left(\frac{P_r}{A_n} \right) \tag{11}$$

When the temperature is high enough (about 200°C) a magnetite layer (Fe_3O_4) is produced on the contact surface [12]. This oxide layer increases the asperities temperature by increasing the resistance to heat flow [20]. In the one-dimensional approximation, the oxide, of thickness Z, contributes an additional (series) resistance to the diffusive path, of length l_f [20], as shown in Fig.3. The l_f is called the equivalent linear diffusion distance for flash heating. The temperature at this l_f distance is the approximately bulk temperature. The r_a is the radius of an asperity. The typical value of

r_a is 10^{-5} (m) [20]. Furthermore the results of layer observation from [12] showed that the thickness of oxide layer on the surface of disc is about 20 (μm). Therefore the l_f can be selected as 20 (μm). As a result, Z is 10 (μm).

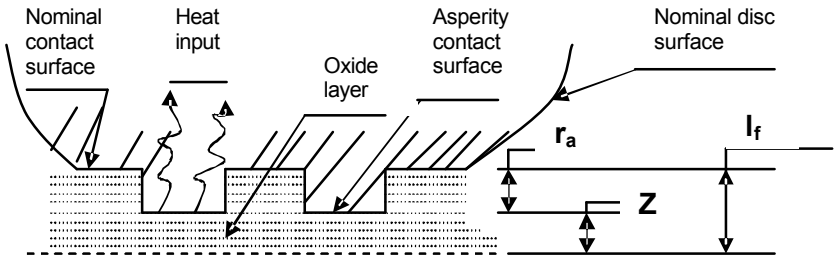

Figure 3: The asperity contact model and the oxide layers on disc surface

As the λ_s and λ_{ox} are the thermal conductivity coefficients of the steel and oxide respectively; and λ_e is the effective thermal conductivity; at steady state, this effective resistance can be attained by summing the resistance of the oxide layer (Z/λ_{ox}) and of the steel ((l_f - Z)/λ_s) as the following equation,

$$\left(l e / l_f\right) = \left(l_s l_{ox}\right) / \left((l_f - Z) l_{ox} + Z l_s\right) \tag{12}$$

With λ_s = 50 (W/m.K) and λ_{ox} = 3.2 (W/m.K), selected from [20]. From (12) $\Rightarrow$ λ_e = 6.0 (W/m.K).

Selecting $\lambda = \lambda_e$; $\rho = \rho_s$ (density of steel) and $C_p = C_{ps}$. Equation (10) becomes,

$$T_f = 17.3\times10^{-5}\left(\frac{a}{V}\right)^{0.5}\frac{P_r}{A_a}, \text{ or, } T_f = 7.1\times10^{-10}\left(\sqrt{p_0}\right)\left(\sqrt{\frac{R}{V_w}}\right)\left(\frac{P_r}{A_n}\right) \tag{13}$$

Equation (13) shows that if the frictional power density, disc radius and rolling velocity do not change, the flash temperature is proportional the contact pressure.

3.2. The relationship between the surface temperature and friction power density

The disc surface temperature (T_{tot}) is the total temperature of the bulk surface temperature and the flash temperature [17] and [20].

When the influence of an oxide layer on the contact surface is neglected, the T_{tot} (^{0}K) can be determined from equations (8), (9) and (11). The relationship between the friction power density and the contact surface temperature can be shown by the following equation.

$$T_{tot} - T_0 = \left(\frac{1.65 + 2.1\times(1+\sqrt{1-x})}{1+\sqrt{1-x}}\right)\left(\sqrt{p_0}\right)\left(\sqrt{\frac{R}{V_w}}\right)\left(\frac{P_r}{A_n}\right)\times10^{-10} \tag{14}$$

$$\text{Or, } \frac{P_r}{A_n} = \left(\frac{1+\sqrt{1-x}}{1.65 + 2.1\times(1+\sqrt{1-x})}\right)\left(\frac{1}{\sqrt{p_0}}\right)\left(\sqrt{\frac{V_w}{R}}\right)\left(T_{tot} - T_0\right)\times10^{10} \tag{15}$$

When the influence of an oxide layer is considered, the flash temperature increases. The T_{tot} is determined from equations (8), (9) and (13). The relationship between the friction power density and contact surface temperature can be given by the following equations.

$$T_{tot} - T_0 = \left(\frac{1.65 + 7.1\times(1+\sqrt{1-x})}{1+\sqrt{1-x}}\right)\left(\sqrt{p_0}\right)\left(\sqrt{\frac{R}{V_w}}\right)\left(\frac{P_r}{A_n}\right)\times10^{-10} \tag{16}$$

$$\text{Or, } \frac{P_r}{A_n} = \left(\frac{1+\sqrt{1-x}}{1.65 + 7.1\times(1+\sqrt{1-x})}\right)\left(\frac{1}{\sqrt{p_0}}\right)\left(\sqrt{\frac{V_w}{R}}\right)\left(T_{tot} - T_0\right)\times10^{10} \tag{17}$$

Equations (14) and (16) showed that the contact surface temperature is proportional to the frictional power density, creep rate, contact pressure and equivalent radius of the contact disc pair; and inversely proportional to the rolling velocity.

4. Discussion

The section will evaluate the analytical models for the wear transitions by comparing their calculation results with the available experiment data in literature.

4.1. Comparison between the calculation result from eq (4) with the experiment results

Based on experimental factors in [1], V = 0.665 (m/s), ξ_0 = 3%, k = 280(MPa) for BS11 and k = 310 (MPa) for 1% chromium rail steel. Using equation (4), E_{I-II} = 4.38 (W/mm^2) for BS11 steel and E_{I-II} = 5.33 (W/mm^2) for 1% chromium steel. These results compare well with the suggested experimental value in [1] and [15] (4W/mm^2 for material pair: steel/steel). Another comparison is shown in table 1, in which the limiting creep rate (ξ_0) is assumed as 3%. Table 1 also shows that the values of E_{I-II} calculated from equation (4) are quite agreement to experiment results in [4].

Table 1: Calculation and Experiment Result for Wear Transition I-II area

Material	Yield stress in simple shear (k) (MPa)	E_{I-II} (W/mm^2), results from eq. (4)	E_{I-II}(W/mm^2), results in [4]
BS11 Rail	380	6	7.9
UICA Rail	426	6.6	9.2
1% Cr Rail	550	8.6	13.2
Class D tyre	405	6.3	8.9

4.2. An evaluation for the analytical model for the second wear transition area

This section compares the temperature calculated from equation (16) with the calculation results from ref. [17], shown in Table 2. Then based on the experimental data in [4], the E_{II-III} and corresponding surface temperatures for some wheel/rail steels will be determined, shown in Table 3.

Table 2 shows that the surface temperatures calculated from equation (16) are higher than that determined from equations in ref. [17], especially in the high creep range. This difference can be explained by the influence of the oxide layer that makes a rise in the flash temperature.

Table 2: Surface temperature for R8T vs. UIC60 900A for p_0 = 1500 (MPa)

Slip (%)	P_r/A_n (W/mm^2)	T_{tot} (^{0}C), Ref. [17]	T_{tot} (^{0}C), Eq. (16)
0.2	0.2	21	21
0.5	1	24	25
1	4	31	34
3	16	64	75
7.5	39	126	151
10	52	161	195
15	78	212	284
20	116	333	411

Table 3: The surface temperature corresponding to the transition area II-III for p_0 =1300 (MPa)

Material	Creepage(%), Ref. [4]	E_{II-III} (W/mm^2)	T_{tot}(^{0}C), Eq. (16)
BS11 Rail	11 –19	25 – 47	130 –223
UICB Rail	16 – 19	38 – 47	187 – 223
UICA Rail	12 – 17	28 – 41	141 – 199
Class D tyre vs. BS11, UICB and UICA	11 – 17	25 – 41	130 – 199
1% Cr Rail	20 – 24	50 – 62	235 – 286
Class D tyre vs. 1% Cr Rail	20	50	235

The experimental investigations for the wear transition in [4] have shown that beyond a creep of 10%, some dramatic changes occurred in the wear rates of both rail and wheel steel. The wear caused by the transition from type II to type III for BS11, UICB, 1% Cr and UICA, occurring in the creep range has been shown, 11%-19%, 16%-19%, 20%-24% and 12%-17% respectively. Based on this data, using equation (16), the surface temperature corresponding to the wear transition is shown in Table 3.

Table 3 shows that for the popular wheel/rail steel (BS11, UICB, UICA), the E_{II-III} is in range from 25 (W/mm^2) to 47 (W/mm^2), corresponding to the surface temperature from 130^{o}C to 223^{o}C. For the special rail steel (such as 1% Chrome rail), E_{II-III} is higher (50 – 62 W/mm^2), corresponding to the higher surface temperature (235 – 286^{o}C). For other steel (such as R8T, in Table 2) E_{II-III} is very high, 78 to 116 (W/mm^2), corresponding to the very high surface temperature (284 – 411^{o}C).

If the main cause of the wear transition between type II and type III is the high temperature that softening the materials, results from Table 3 showed that these temperature ranges are quite different for the different wheel/rail steels. Furthermore when the temperature range softening wheel/rail steels are known, the values E_{II-III} can be determined by equation (17).

5. Conclusions

An analytical model (equation (4)) for determination of the wear transition area between wear type I and type II has been suggested. The calculated results from this equation corroborate with the available experiment results in literature.

The relationship between the friction power density and contact surface temperature in twin-disc contact was described by the analytical equations (14), (15), (16) and (17). These equations may be useful tools to investigate the wear transition area between type II and type III wear.

Tests for the first wear transition have being carried out to calibrate the suggested analytical model.

References

[1] T.M. Beagley, Severe Wear of Rolling/Sliding Contacts, Wear 36 (1976) 317-335.

[2] K.O. Bjorn, New approach for predicting wheel profile wear, 7th International Conference on Contact Mechanics and Wear of Rail/Wheel Systems (CM2006), Australia, 2006 (2006).

[3] H. Blok, The flash temperature concept, Wear 6 (1963) 483-494.

[4] P.J. Bolton, P. Clayton, Rolling-Sliding Wear Damage in Rail and Tyre steels, Wear 93 (1984) 145-165.

[5] F. Braghin, R. Lewis, R.S. Dwyer-Joyce, S. Bruni, A Mathematical Model to Predict Railway Wheel Profile Evolution due to Wear, Wear (2006) (in Press).

[6] B.S.M.C. Commitee, BSCC High Temperature Data, The Iron and Steel Institute for the BSCC, London (1973).

[7] D. Danks, P. Clayton, Comparison of the Wear Process For Eutectoid Rail Steel: Field and Laboratory Tests, Wear 120 (1987) 233-250.

[8] D.T. Eadie, Elvidge, D., Oldknow, K., Stock, R., Pointner, P., Kalousek, J., Klauser, P., The effects of top of rail friction modifier on wear and rolling contact fatigue: full scale rail-wheel testrig evaluation, analysis and modelling, 7th International Conference on Contact Mechanics and Wear of Rail/Wheel System (CM2006), Brisbane, Australia, September 24-26, 2006 (2006).

[9] M. Ertz., K. Knothe, A comparison of analytical and numerical methods for the calculation of temperature in wheel/rail contact, Wear 253 (2002) 498-508.

[10] S. Fouvry, Shakedown analysis and fretting wear response under gross slip condition, Wear 251 (2001) 1320-1331.

[11] S. Fouvry, P. Kapsa, L. Vincent, An elastic-plastic shakedown analysis of fretting wear, Wear 247 (2001) 41-54.

[12] K. Hou, J. Kalousek, E. Mangel, Rheological model of solid layer in rolling contact, Wear 211 (1997) 134 - 140.

[13] K.L. Johnson, Contact mechanics (Cambridge University Press, Cambridge, 1999).

[14] K.L. Johnson, Contact mechanics and the wear of matals, Wear 190 (1995) 162-170.

[15] H. Klause, G. Poll, Wear of Wheel-Rail Surface, Wear 113 (1986) 103-122.

[16] K. Knothe, S. Liebelt, Determination of temperatures for sliding contact with application for wheel-rail system, Wear 189 (1995) 91-99.

[17] R. Lewis, R.S. Dwyer-Joyce, Wear mechanisms and transitions in railway wheel steels, Proc Instn Mech Engrs Part J. Engineering Tribology 218 (2004) 467-478.

[18] R. Lewis, R.S. Dwyer-Joyce, U. Olofsson, R.I. Hallam, Wheel material wear mechanisms and transitions, Paper from 14th International wheelset congress, Orlando, USA (2001).

[19] R.B. Lewis, U. Olofsson, Mapping Rail Wear Regimes and Transitions, Wear 257 (2004) 721-729.

[20] S.C. Lim, M.F. Ashby, Wear-Mechanism Maps, Acta Metal 35 (1987) 1-24.

[21] R. Nakkalil, J.R. Hornaday, M. Nabil Bassim, Characterization of the compression properties of rail steels at high temperature and strain rates, Materials Science and Engineering A141 (1991) 247-260.

[22] T.T. Vuong, P.A. Meehan, A literature survey of wear coefficient used for studying the wheel/rail wear, Research Report No: 2007/05, Department of Mechanical Engineering, The University of Queensland, Australia.

[23] I. Zobory, Prediction of wheel/rail profile wear, Vehicle System Dynamics 28 (1997) 221-259.